*mathematics*

MDPI

*Article*

# Exploring the Diversity of Kink Solitons in (3+1)-Dimensional Wazwaz–Benjamin–Bona–Mahony Equation

**Musawa Yahya Almusawa * and Hassan Almusawa**

Department of Mathematics, Faculty of Science, Jazan University, P.O. Box 2097, Jazan 45142, Saudi Arabia; haalmusawa@jazanu.edu.sa

* Correspondence: malmusawi@jazanu.edu.sa

**Abstract:** The Wazwaz–Benjamin–Bona–Mahony (WBBM) equation is a well-known regularized long-wave model that examines the propagation kinematics of water waves. The current work employs an effective approach, called the Riccati Modified Extended Simple Equation Method (RMESEM), to effectively and precisely derive the propagating soliton solutions to the (3+1)-dimensional WBBM equation. By using this upgraded approach, we are able to find a greater diversity of families of propagating soliton solutions for the WBBM model in the form of exponential, rational, hyperbolic, periodic, and rational hyperbolic functions. To further graphically represent the propagating behavior of acquired solitons, we additionally provide 3D, 2D, and contour graphics which clearly demonstrate the presence of kink solitons, including solitary kink, anti-kink, twinning kink, bright kink, bifurcated kink, lump-like kink, and other multiple kinks in the realm of WBBM. Furthermore, by producing new and precise propagating soliton solutions, our RMESEM demonstrates its significance in revealing important details about the model behavior and provides indications regarding possible applications in the field of water waves.

**Keywords:** nonlinear partial differential equations; (3+1)-dimensional Wazwaz–Benjamin–Bona–Mahony equation; Riccati modified extended simple equation method; kink solitons; long waves

**MSC:** 32G34; 32W50; 34B15; 93C20

check for updates

**Citation:** Almusawa, M.Y.; Almusawa, H. Exploring the Diversity of Kink Solitons in (3+1)-Dimensional Wazwaz–Benjamin–Bona–Mahony Equation. *Mathematics* **2024**, *12*, 3340. https://doi.org/10.3390/math12213340

Academic Editors: Teng Huang, Qiong Wang and Yan Pang

Received: 10 September 2024
Revised: 22 October 2024
Accepted: 23 October 2024
Published: 24 October 2024

**Copyright:** © 2024 by the authors. Licensee MDPI, Basel, Switzerland. This article is an open access article distributed under the terms and conditions of the Creative Commons Attribution (CC BY) license (https://creativecommons.org/licenses/by/4.0/).

## 1. Introduction

Nonlinear Partial Differential Equations (NPDEs) possess applications in numerous fields of mathematics, engineering and physics. These frameworks efficiently explain a broad range of phenomena, including thermal conductivity, the dispersion of organic compounds, fluid mechanics, wave bending, magnetism, quantum field theory, hydrodynamics, and oceanic wave propagation. These NPDEs include renowned models such as Burgers' equation, the Fisher equation, the Boussinesq equation, the advection equation, and other coupled nonlinear equations [1–5].

Among the aforementioned nonlinear models, several well-known equations have been studied in detail in relation to NPDEs, including the regularized long-wave model, the modified Korteweg–de Vries (KdV) model and the Boussinesq model [6,7]. Benjamin, Bona, and Mahony initially presented the KdV model in 1972 to characterize wave motion below the surface in a homogeneous channel. This led to the development of the normalized KdV model known as the Benjamin–Bona–Mahony (BBM) model, which focuses on shallow wave propagation. The BBM model is used to analyse drifting waves and Rossby waves in rotating fluid systems [8–10]. The BBM model is provided as [11]

$$Q_t + Q_x + Q^n Q_x - Q_{xxt} = 0, \tag{1}$$

while the KdV model is articulated as [12]

$$Q_t + Q_x + QQ_x + Q_{xxx} = 0, \tag{2}$$

where the function $Q = Q(x, t)$ expresses the displacement of the surface of a fluid from its rest state or wave height. Moreover, the linear terms account for the propagation of wave, the $Q_{xxt}$ and $Q_{xxx}$ signify the dispersive terms, and the nonlinear term $Q^n Q_x$ represents wave interaction. A variety of waves, including surface pulses in water, prolonged signals in acoustic energy in periodic pebbles, nonlinear diffraction workflows, magnetic hydrodynamic waves in erythrocytes, and reverberating waves in compressible fluids, are modeled using the BBM equation and the KdV equation [13]. However, there are several notable differences between these two equations. The BBM equation and the KdV equation are equivalent only when low-frequency waves are considered, and the findings they yield about waves diverge. While the BBM equation is categorized as a regularity equation, the KdV equation serves as an existence equation [14]. The theory of the BBM model, including its uniqueness, stability, and consistency, is investigated in [15,16]. The BBM model has additionally been the focus of a great deal of research in recent years. There is general agreement that the BBM model is much simpler to solve than the KdV model; nonetheless, both equations possess stable solutions for single waves [17,18]. Sometimes the long-wave equation is used instead of the BBM equation. When $n = 2$, the BBM equation in Equation (1) changes to the modified BBM equation. Ref. [19] investigated the solutions to a number of issues, including the modified BBM model starting values.

A novel equation for describing the three-dimensional kinematics of water waves was proposed by Wazwaz in 2017 [20]. A variation of the Benjamin–Bona–Mahony equation is the WBBM equation. Consequently, Wazwaz assessed the subsequent manufacturer equations:

$$\begin{aligned} &Q_t + Q_x + Q^2 Q_y - Q_{xzt} = 0, \\ &Q_t + Q_z + Q^2 Q_x - Q_{xyt} = 0, \\ &Q_t + Q_y + Q^2 Q_z - Q_{xxt} = 0, \end{aligned} \tag{3}$$

where $Q = Q(t, x, y, z)$ is the differentiable functions that represent the amplitude of the wave function in the equation. The three-dimensional WBBM model, which is expressed as follows, is the main topic of this study:

$$Q_t + Q_x + (Q^3)_y - Q_{xzt} = 0. \tag{4}$$

In the literature, a plethora of numerical and analytical methods have been developed to address NPDEs. Despite the availability of numerical tools, analysts often opt for analytical methods because they may offer a comprehensive grasp of the underlying physical processes and accurate insights into the system's behavior. Analytical solutions for NPDEs are, nevertheless, hard to find. Consequently, research into creating analytical treatments for NPDEs is still crucial. Various analytical techniques have been developed to address this problem. The Khater method [21], Adomian decomposition method [22], (G′/G)-expansion method [23], variable separable method [24], Exp-function method [25], integral transforms method [26], homotopy perturbation method [27], differential transform method [28], Extended Direct Algebraic Method (EDAM) [29], and numerous others [30–32] are a few of these approaches. This method involves converting the NPDEs into Nonlinear Ordinary Differential Equations (NODEs) using variable transformation. Next, the NODEs are assumed to have a closed-form solution and are converted into systems of algebraic equations. The resulting system of algebraic equations may be solved to provide the soliton solutions for the appropriate NPDEs. The soliton solutions generated by RMESEM can aid in our comprehension of the system's behavior and underlying physical processes.

This work utilizes the strategic RMESEM for swiftly and correctly obtaining propagating soliton solutions to the (3+1)-dimensional WBBM problem. By using this updated

approach, we are able to find a large number of families of propagating soliton solutions for the WBBM model in the form of exponential, rational, hyperbolic, periodic, and rational hyperbolic functions. We also offer 3D, 2D, and contour graphics to further graphically depict the propagating behavior of the acquired solitons. These graphics clearly show the existence of kink solitons, such as anti-kink, twinning kink, bright kink, bifurcated kink, lump-like kink, and other multiple kinks in the context of WBBM. Furthermore, by producing new and accurate propagating soliton solutions, our employed RMESEM demonstrates its value in revealing important details about the equation dynamics and provides indications regarding possible applications in the field of water waves.

The remaining paperwork is organized as follows: The working mechanism of the RMESEM is explained in Section 2, the WBBM model is addressed in Section 3 to create new soliton solutions, the propagating behavior of kink solitons is visually shown in Section 4, the results are summarized in Section 5, and the final section presents Appendix A.

## 2. The Methodical Strategy of RMESEM

The literature has established a wide range of analytical methods to study soliton occurrences in nonlinear models [33–35]. In this part, we describe the operation mechanism of the improved RMESEM [36]. Examining the upcoming NLPDE,

$$F(Q, Q_t, Q_{\tau_1}, Q_{\tau_2}, QQ_{\tau_1}, \dots) = 0, \tag{5}$$

where $Q = Q(t, \tau_1, \tau_2, \tau_3, \dots, \tau_r)$.

Equation (5) is to be solved using the following steps:

1. First, a variable-form wave transformation $Q(t, \tau_1, \tau_2, \tau_3, \dots, \tau_r) = P(\phi)$ is carried out. There are several definitions to represent $\phi$. Through this transformation, Equation (5) is modified to obtain the following NODE:

$$G(P, P'P, P', \dots) = 0, \tag{6}$$

where $P' = \frac{dP}{d\phi}$. On occasion, the NODE may be made to comply with the homogeneous balance requirement by using integrating Equation (6).

2. Next, we suppose a series-based solution with the help of the solution to the extended Riccati ODE to solve the NODE in (6) [36]:

$$P(\phi) = \sum_{m=0}^{p} m_j \left(\frac{\Upsilon'(\phi)}{\Upsilon(\phi)}\right)^j + \sum_{j=0}^{p-1} s_j \left(\frac{\Upsilon'(\phi)}{\Upsilon(\phi)}\right)^j \cdot \left(\frac{1}{\Upsilon(\phi)}\right). \tag{7}$$

Here, the solution to the resultant extended Riccati ODE is denoted by $\Upsilon(\phi)$ [36], and the unknown constants that need to be found later are represented by the parameters $m_j (j = 0, ..., p)$ and $s_j (j = 0, ..., p-1)$.

$$\Upsilon'(\phi) = J + K\Upsilon(\phi) + L(\Upsilon(\phi))^2, \tag{8}$$

where $J, K$ and $L$ are constants.

3. The positive integer $p$ needed in Equation (7) is obtained by homogeneously balancing the highest-order derivative term and the largest nonlinear term in Equation (6).

4. Afterwards, all the terms with the same powers of $\Upsilon(\phi)$ are combined when (7) is substituted into (6) or in the equation that emerges from the integration of (6). This procedure results in an equation in terms of $\Upsilon(\phi)$. By setting the coefficients in this equation to zero, we generate an algebraic system of equations representing the parameters $m_j (j = 0, ..., p)$ and $s_j (j = 0, ..., p-1)$ along with the further associated parameters.

5. Using MAPLE, an analytical treatment of the resultant set of nonlinear algebraic equations is carried out.

6. Afterwards, analytical soliton solutions for (5) are produced by computing and entering the unknown values in Equation (7) together with $\Upsilon(\phi)$ (Equation (8) solution).

Several families of soliton solutions may be derived by using the general solution of (8). These are displayed in Table 1 [36].

**Table 1.** The particular solutions $\Upsilon(\phi)$ of the Riccati equation in (8) and the formation of $\left(\frac{\Upsilon'(\phi)}{\Upsilon(\phi)}\right)$, where $n_1, n_2 \in \mathrm{R}$, $\varpi = K^2 - 4LJ$ and $\zeta = \cosh\left(\frac{1}{4}\sqrt{\varpi}\phi\right)\sinh\left(\frac{1}{4}\sqrt{\varpi}\phi\right)$.

| S. No. | Family | Constraint(s) | $\Upsilon(\phi)$ | $\left(\frac{\Upsilon'(\phi)}{\Upsilon(\phi)}\right)$ |
|---|---|---|---|---|
| 1 | Trigonometric Solutions | $\varpi < 0, \quad L \neq 0$ | $-\frac{K}{2L} + \frac{\sqrt{-\varpi}\tan\left(\frac{1}{2}\sqrt{-\varpi}\phi\right)}{2L}$, | $-\frac{\varpi\left(1+\left(\tan\left(\frac{1}{2}\sqrt{-\varpi}\phi\right)\right)^2\right)}{2(-K+\sqrt{-\varpi}\tan\left(\frac{1}{2}\sqrt{-\varpi}\phi\right))}$, |
| | | | $-\frac{K}{2L} - \frac{\sqrt{-\varpi}\cot\left(\frac{1}{2}\sqrt{-\varpi}\phi\right)}{2L}$, | $\frac{\left(1+\left(\cot\left(\frac{1}{2}\sqrt{-\varpi}\phi\right)\right)^2\right)\varpi}{2(K+\sqrt{-\varpi}\cot\left(\frac{1}{2}\sqrt{-\varpi}\phi\right))}$, |
| | | | $-\frac{K}{2L} + \frac{\sqrt{-\varpi}\left(\tan\left(\sqrt{-\varpi}\phi\right)+\left(\sec\left(\sqrt{-\varpi}\phi\right)\right)\right)}{2L}$, | $\frac{-\varpi\left(1+\sin\left(\sqrt{-\varpi}\phi\right)\right)\sec\left(\sqrt{-\varpi}\phi\right)}{-K\cos\left(\sqrt{-\varpi}\phi\right)+\sqrt{-\varpi}\sin\left(\sqrt{-\varpi}\phi\right)+\sqrt{-\varpi}}$, |
| | | | $-\frac{K}{2L} + \frac{\sqrt{-\varpi}\left(\tan\left(\sqrt{-\varpi}\phi\right)-\left(\sec\left(\sqrt{-\varpi}\phi\right)\right)\right)}{2L}$. | $\frac{\varpi\left(\sin\left(\sqrt{-\varpi}\phi\right)-1\right)\sec\left(\sqrt{-\varpi}\phi\right)}{-K\cos\left(\sqrt{-\varpi}\phi\right)+\sqrt{-\varpi}\sin\left(\sqrt{-\varpi}\phi\right)-\sqrt{-\varpi}}$. |
| 2 | Hyperbolic Solutions | $\varpi > 0, \quad L \neq 0$ | $-\frac{K}{2L} - \frac{\sqrt{\varpi}\tanh\left(\frac{1}{2}\sqrt{\varpi}\phi\right)}{2L}$, | $-\frac{\left(-1+\left(\tanh\left(\frac{1}{2}\sqrt{\varpi}\phi\right)\right)^2\right)\varpi}{2(K+\sqrt{\varpi}\tanh\left(\frac{1}{2}\sqrt{\varpi}\phi\right))}$, |
| | | | $-\frac{K}{2L} - \frac{\sqrt{\varpi}\left(\tanh\left(\sqrt{\varpi}\phi\right)+i\left(\mathrm{sech}\left(\sqrt{\varpi}\phi\right)\right)\right)}{2L}$, | $\frac{-\varpi\left(-1+i\sinh\left(\sqrt{\varpi}\phi\right)\right)\mathrm{sech}\left(\sqrt{\varpi}\phi\right)}{K\cosh\left(\sqrt{\varpi}\phi\right)+\sqrt{\varpi}\sinh\left(\sqrt{\varpi}\phi\right)+i\sqrt{\varpi}}$, |
| | | | $-\frac{K}{2L} - \frac{\sqrt{\varpi}\left(\tanh\left(\sqrt{\varpi}\phi\right)-i\left(\mathrm{sech}\left(\sqrt{\varpi}\phi\right)\right)\right)}{2L}$, | $\frac{-\varpi\left(1+i\sinh\left(\sqrt{\varpi}\phi\right)\right)\mathrm{sech}\left(\sqrt{\varpi}\phi\right)}{-K\cosh\left(\sqrt{\varpi}\phi\right)-\sqrt{\varpi}\sinh\left(\sqrt{\varpi}\phi\right)+i\sqrt{\varpi}}$, |
| | | | $-\frac{K}{2L} - \frac{\sqrt{\varpi}\left(\coth\left(\sqrt{\varpi}\phi\right)+\left(\mathrm{csch}\left(\sqrt{\varpi}\phi\right)\right)\right)}{2L}$. | $-\frac{\varpi\left(2\left(\cosh\left(\frac{1}{4}\sqrt{\varpi}\phi\right)\right)^2-1\right)}{4\zeta\left(-2K\zeta+\sqrt{\varpi}\right)}$. |
| 3 | Rational Solutions | $\varpi = 0$ | $\frac{-2J(K\phi+2)}{K^2\phi}$, | $\frac{-2}{\phi(K\phi+2)}$, |
| | | $\varpi = 0$, & $K = L = 0$ | $\phi J$, | $\frac{1}{\phi}$, |
| | | $\varpi = 0$, & $K = J = 0$ | $-\frac{1}{\phi L}$. | $-\frac{1}{\phi}$. |
| 4 | Exponential Solutions | $L = 0$, & $K = \epsilon, J = \kappa\epsilon$ | $e^{\epsilon\phi} - \kappa$, | $\frac{\epsilon e^{\epsilon\phi}}{e^{\epsilon\phi}-\kappa}$, |
| | | $J = 0$, & $K = \epsilon, L = \kappa\epsilon$ | $\frac{e^{\epsilon\phi}}{1-\kappa e^{\epsilon\phi}}$. | $-\frac{\epsilon}{-1+\kappa e^{\epsilon\phi}}$. |
| 5 | Rational-Hyperbolic Solutions | $J = 0$, & $K \neq 0, L \neq 0$ | $-\frac{Kn_1}{L(\cosh(K\phi)-\sinh(K\phi)+n_2)}$, | $\frac{K(\sinh(K\phi)-\cosh(K\phi))}{-\cosh(K\phi)+\sinh(K\phi)-n_2}$, |
| | | | $-\frac{K(\cosh(K\phi)+\sinh(K\phi))}{L(\cosh(K\phi)+\sinh(K\phi)+n_2)}$. | $\frac{Kn_2}{\cosh(K\phi)+\sinh(K\phi)+n_2}$. |

## 3. The Construction of Kink Soliton Solutions for WBBM

In this section, we apply our suggested approach, RMESEM, to acquire families of the soliton solutions for WBBM given in (4). We begin with the application of the transformation that follows:

$$Q(t,x,y,z) = P(\phi), \quad \text{where} \quad \phi = \lambda x + \mu y + \nu z - \omega t. \tag{9}$$

By appending (9) to it, (4) now becomes

$$(\lambda - \omega)P' + \mu(P^3)' + \nu\lambda\omega P''' = 0, \tag{10}$$

where $P' = \frac{dP}{d\phi}$. According to the homogeneous balancing principle, $p = 1$ is suggested by balancing the greatest derivative $\nu\lambda\omega P'''$ and the largest nonlinear term $\mu(P^3)'$. Putting $p = 1$ in (7) yields the following solution for (10):

$$P(\phi) = \sum_{m=0}^{1} m_j \left(\frac{\Upsilon'(\phi)}{\Upsilon(\phi)}\right)^j + s_0\left(\frac{1}{\Upsilon(\phi)}\right), \tag{11}$$

where the constants $s_1$, $m_0$, and $m_1$ are unknown. When we insert (11) into (10), we obtain an expression in $\Upsilon(\phi)$. An algebraic system of seven equations may be obtained by gathering all terms with the same powers of $\Upsilon(\phi)$ and setting the coefficient of each term to zero. We solve the system with Maple. And as a result, the system of algebraic equations yields the following five cases of results.
Case. 1

$$m_0 = \frac{s_0 K}{2J}, m_1 = 0, s_0 = s_0, \lambda = \lambda, \mu = \frac{-4J^2(-\omega+\lambda)}{\varpi\, {s_0}^2}, \nu = \frac{2(\lambda-\omega)}{\lambda\,\omega\,\varpi}, \omega = \omega. \tag{12}$$

Case. 2

$$m_0 = m_0, m_1 = m_1, s_0 = s_0, \lambda = \omega, \mu = 0, \nu = 0, \omega = \omega. \tag{13}$$

Case. 3

$$m_0 = -\frac{m_1 K}{2}, m_1 = m_1, s_0 = 0, \lambda = \lambda, \mu = \frac{-4(\lambda-\omega)}{(8\,JL+K^2){m_1}^2}, \nu = \frac{2(\lambda-\omega)}{\lambda\,\omega\,(8\,JL+K^2)}, \omega = \omega. \tag{14}$$

Case. 4

$$m_0 = -\frac{m_1 K}{2}, m_1 = m_1, s_0 = -m_1 J, \lambda = \lambda, \mu = \frac{-4(\lambda-\omega)}{\varpi\, {m_1}^2}, \nu = \frac{2(\lambda-\omega)}{\lambda\,\omega\,\varpi}, \omega = \omega. \tag{15}$$

Taking into consideration **Case. 1** and utilizing (9) and (11) with the corresponding solution of (8), we acquire the ensuing families of kink soliton solutions for (4):
Family. 1.1: When $\varpi < 0 \quad L \neq 0$,

$$Q_{1,1}(t,x,y,z) = \frac{s_0 K}{2J} + s_0\left(-\frac{K}{2L} + \frac{\sqrt{-\varpi}\tan\left(\frac{1}{2}\sqrt{-\varpi}\phi\right)}{2L}\right)^{-1}, \tag{16}$$

$$Q_{1,2}(t,x,y,z) = \frac{s_0 K}{2J} + s_0\left(-\frac{K}{2L} - \frac{\sqrt{-\varpi}\cot\left(\frac{1}{2}\sqrt{-\varpi}\phi\right)}{2L}\right)^{-1}, \tag{17}$$

$$Q_{1,3}(t,x,y,z) = \frac{s_0 K}{2J} + s_0\left(-\frac{K}{2L} + \frac{\sqrt{-\varpi}\left(\tan\left(\sqrt{-\varpi}\phi\right) + \sec\left(\sqrt{-\varpi}\phi\right)\right)}{2L}\right)^{-1}, \tag{18}$$

and

$$Q_{1,4}(t,x,y,z) = \frac{s_0 K}{2J} + s_0\left(-\frac{K}{2L} + \frac{\sqrt{-\varpi}\left(\tan\left(\sqrt{-\varpi}\phi\right) - \sec\left(\sqrt{-\varpi}\phi\right)\right)}{2L}\right)^{-1}. \tag{19}$$

Family. 1.2: When $\varpi > 0 \quad L \neq 0$,

$$Q_{1,5}(t,x,y,z) = \frac{s_0 K}{2J} + s_0\left(-\frac{K}{2L} - \frac{\sqrt{\varpi}\tanh\left(\frac{1}{2}\sqrt{\varpi}\phi\right)}{2L}\right)^{-1}, \tag{20}$$

$$Q_{1,6}(t,x,y,z) = \frac{s_0K}{2J} + s_0\left(-\frac{K}{2L} - \frac{\sqrt{\varpi}\left(\tanh\left(\sqrt{\varpi}\phi\right) + i\mathrm{sech}\left(\sqrt{\varpi}\phi\right)\right)}{2L}\right)^{-1}, \tag{21}$$

$$Q_{1,7}(t,x,y,z) = \frac{s_0K}{2J} + s_0\left(-\frac{K}{2L} - \frac{\sqrt{\varpi}\left(\tanh\left(\sqrt{\varpi}\phi\right) - i\mathrm{sech}\left(\sqrt{\varpi}\phi\right)\right)}{2L}\right)^{-1}, \tag{22}$$

and

$$Q_{1,8}(t,x,y,z) = \frac{s_0K}{2J} + s_0\left(-\frac{K}{2L} - \frac{\sqrt{\varpi}\left(\tanh\left(\frac{1}{4}\sqrt{\varpi}\phi\right) - \coth\left(\frac{1}{4}\sqrt{\varpi}\phi\right)\right)}{4L}\right)^{-1}. \tag{23}$$

Family. 1.3: When $K = \epsilon$, $J = \kappa\epsilon(\kappa \neq 0)$ and $L = 0$,

$$Q_{1,9}(t,x,y,z) = \frac{s_0}{2\kappa} + \frac{s_0}{e^{\epsilon\,\phi} - \kappa}. \tag{24}$$

In the above kink soliton solutions, $\phi = \lambda x + (\frac{J^2(-4(\lambda-\omega))}{\varpi\, {s_0}^2})y + (\frac{2(\lambda-\omega)}{\lambda\,\omega\,\varpi})z - \omega t$.

Taking into consideration **Case. 2** and utilizing (9) and (11) with the corresponding solution of (8), we acquire the ensuing families of kink soliton solutions for (4):
Family. 2.1: When $\varpi < 0 \quad L \neq 0$,

$$Q_{2,1}(t,x,y,z) = m_0 + \frac{m_1\varpi\left(1 + \left(\tan\left(\frac{1}{2}\sqrt{-\varpi}\phi\right)\right)^2\right)}{2(K - \sqrt{-\varpi}\tan\left(\frac{1}{2}\sqrt{-\varpi}\phi\right))} + s_0\left(-\frac{K}{2L} + \frac{\sqrt{-\varpi}\tan\left(\frac{1}{2}\sqrt{-\varpi}\phi\right)}{2L}\right)^{-1}, \tag{25}$$

$$Q_{2,2}(t,x,y,z) = m_0 + \frac{m_1\varpi\left(1 + \left(\tan\left(\frac{1}{2}\sqrt{-\varpi}\phi\right)\right)^2\right)}{2(K - \sqrt{-\varpi}\tan\left(\frac{1}{2}\sqrt{-\varpi}\phi\right))} + s_0\left(-\frac{K}{2L} + \frac{\sqrt{-\varpi}\tan\left(\frac{1}{2}\sqrt{-\varpi}\phi\right)}{2L}\right)^{-1}, \tag{26}$$

$$\begin{aligned} Q_{2,3}(t,x,y,z) =& \frac{m_1\varpi\left(1 + \sin\left(\sqrt{-\varpi}\phi\right)\right)}{\cos\left(\sqrt{-\varpi}\phi\right)\left(K\cos\left(\sqrt{-\varpi}\phi\right) - \sqrt{-\varpi}\sin\left(\sqrt{-\varpi}\phi\right) - \sqrt{-\varpi}\right)} \\ &+ s_0\left(-\frac{K}{2L} + \frac{\sqrt{-\varpi}\left(\tan\left(\sqrt{-\varpi}\phi\right) + \sec\left(\sqrt{-\varpi}\phi\right)\right)}{2L}\right)^{-1} + m_0, \end{aligned} \tag{27}$$

and

$$\begin{aligned} Q_{2,4}(t,x,y,z) =& -\frac{m_1\varpi\left(\sin\left(\sqrt{-\varpi}\phi\right) - 1\right)}{\cos\left(\sqrt{-\varpi}\phi\right)\left(K\cos\left(\sqrt{-\varpi}\phi\right) - \sqrt{-\varpi}\sin\left(\sqrt{-\varpi}\phi\right) + \sqrt{-\varpi}\right)} \\ &+ s_0\left(-\frac{K}{2L} + \frac{\sqrt{-\varpi}\left(\tan\left(\sqrt{-\varpi}\phi\right) - \sec\left(\sqrt{-\varpi}\phi\right)\right)}{2L}\right)^{-1} + m_0. \end{aligned} \tag{28}$$

Family. 2.2: When $\varpi > 0 \quad L \neq 0$,

$$Q_{2,5}(t,x,y,z) = m_0 - \frac{1}{2}\frac{m_1\varpi\left(-1 + \left(\tanh\left(\frac{1}{2}\sqrt{\varpi}\phi\right)\right)^2\right)}{K + \sqrt{\varpi}\tanh\left(\frac{1}{2}\sqrt{\varpi}\phi\right)} + s_0\left(-\frac{K}{2L} - \frac{\sqrt{\varpi}\tanh\left(\frac{1}{2}\sqrt{\varpi}\phi\right)}{2L}\right)^{-1}, \tag{29}$$

$$\begin{aligned} Q_{2,6}(t,x,y,z) =& -\frac{m_1\varpi\left(-1+i\sinh\left(\sqrt{\varpi}\phi\right)\right)}{\cosh\left(\sqrt{\varpi}\phi\right)\left(K\cosh\left(\sqrt{\varpi}\phi\right)+\sqrt{\varpi}\sinh\left(\sqrt{\varpi}\phi\right)+i\sqrt{\varpi}\right)} \\ &+ s_0\left(-\frac{K}{2L}-\frac{\sqrt{\varpi}\left(\tanh\left(\sqrt{\varpi}\phi\right)+i\mathrm{sech}\left(\sqrt{\varpi}\phi\right)\right)}{2L}\right)^{-1}+m_0, \end{aligned} \tag{30}$$

$$\begin{aligned} Q_{2,7}(t,x,y,z) =& \frac{m_1\varpi\left(1+i\sinh\left(\sqrt{\varpi}\phi\right)\right)}{\cosh\left(\sqrt{\varpi}\phi\right)\left(K\cosh\left(\sqrt{\varpi}\phi\right)+\sqrt{\varpi}\sinh\left(\sqrt{\varpi}\phi\right)-i\sqrt{\varpi}\right)} \\ &+ s_0\left(-\frac{K}{2L}-\frac{\sqrt{\varpi}\left(\tanh\left(\sqrt{\varpi}\phi\right)-i\mathrm{sech}\left(\sqrt{\varpi}\phi\right)\right)}{2L}\right)^{-1}+m_0, \end{aligned} \tag{31}$$

and

$$\begin{aligned} Q_{2,8}(t,x,y,z) =& \frac{1}{4}\frac{m_1\varpi\left(2\left(\cosh\left(\frac{1}{4}\sqrt{\varpi}\phi\right)\right)^2-1\right)}{\cosh\left(\frac{1}{4}\sqrt{\varpi}\phi\right)\sinh\left(\frac{1}{4}\sqrt{\varpi}\phi\right)\left(2K\cosh\left(\frac{1}{4}\sqrt{\varpi}\phi\right)\sinh\left(\frac{1}{4}\sqrt{\varpi}\phi\right)-\sqrt{\varpi}\right)} \\ &+ s_0\left(-\frac{K}{2L}-\frac{\sqrt{\varpi}\left(\tanh\left(\frac{1}{4}\sqrt{\varpi}\phi\right)-\coth\left(\frac{1}{4}\sqrt{\varpi}\phi\right)\right)}{4L}\right)^{-1}+m_0. \end{aligned} \tag{32}$$

Family. 2.3: When $\varpi = 0, \quad K \neq 0$,

$$Q_{2,9}(t,x,y,z) = m_0 - \frac{2m_1}{\phi\left(K\phi+2\right)} - \frac{s_0K^2\phi}{2J(K\phi+2)}. \tag{33}$$

Family. 2.4: When $\varpi = 0$, in case when $K = L = 0$,

$$Q_{2,10}(t,x,y,z) = m_0 + \frac{m_1}{\phi} + \frac{s_0}{J\phi}. \tag{34}$$

Family. 2.5: When $\varpi = 0$, in case when $K = J = 0$,

$$Q_{2,11}(t,x,y,z) = m_0 - \frac{m_1}{\phi} - s_0L\phi. \tag{35}$$

Family. 2.6: When $K = \epsilon$, $J = \kappa\epsilon(\kappa \neq 0)$ and $L = 0$,

$$Q_{2,12}(t,x,y,z) = m_0 + \frac{m_1\epsilon\,\mathrm{e}^{\epsilon\,\phi}}{\mathrm{e}^{\epsilon\,\phi}-\kappa} + \frac{s_0}{\mathrm{e}^{\epsilon\,\phi}-\kappa}. \tag{36}$$

**Family. 2.7**: When $K = \epsilon$, $L = \kappa\epsilon(\kappa \neq 0)$ and $J = 0$,

$$Q_{2,13}(t,x,y,z) = m_0 - \frac{m_1\epsilon}{-1+\kappa\,\mathrm{e}^{\epsilon\,\phi}} + \frac{s_0\left(1-\kappa\,\mathrm{e}^{\epsilon\,\phi}\right)}{\mathrm{e}^{\epsilon\,\phi}}. \tag{37}$$

Family. 2.8: When $J = 0$, $L \neq 0$ and $K \neq 0$,

$$Q_{2,14}(t,x,y,z) = m_0 + \frac{m_1K(\sinh(K\phi)-\cosh(K\phi))}{-\cosh(K\phi)+\sinh(K\phi)-n_2} - \frac{s_0L(\cosh(K\phi)-\sinh(K\phi)+n_2)}{n_1K}, \tag{38}$$

and

$$Q_{2,15}(t,x,y,z) = m_0 + \frac{m_1Kn_2}{\cosh(K\phi)+\sinh(K\phi)+n_2} - \frac{s_0L(\cosh(K\phi)+\sinh(K\phi)+n_2)}{K(\cosh(K\phi)+\sinh(K\phi))}. \tag{39}$$

In the above kink soliton solutions, $\phi = \lambda(x - t)$.

Taking into consideration **Case. 3** and utilizing (9) and (11) with the corresponding solution of (8), we acquire the ensuing families of kink soliton solutions for (4):

Family. 3.1: When $\varpi < 0 \quad L \neq 0$,

$$Q_{3,1}(t,x,y,z) = -\frac{m_1 K}{2} + \frac{m_1 \varpi \left(1 + \left(\tan\left(\frac{1}{2}\sqrt{-\varpi}\phi\right)\right)^2\right)}{2(K - \sqrt{-\varpi}\tan\left(\frac{1}{2}\sqrt{-\varpi}\phi\right))}, \tag{40}$$

$$Q_{3,2}(t,x,y,z) = -\frac{m_1 K}{2} + \frac{m_1 \varpi \left(1 + \left(\cot\left(\frac{1}{2}\sqrt{-\varpi}\phi\right)\right)^2\right)}{2(K + \sqrt{-\varpi}\cot\left(\frac{1}{2}\sqrt{-\varpi}\phi\right))}, \tag{41}$$

$$Q_{3,3}(t,x,y,z) = -\frac{m_1 K}{2} + \frac{m_1 \varpi \left(1 + \sin\left(\sqrt{-\varpi}\phi\right)\right)}{\cos\left(\sqrt{-\varpi}\phi\right)\left(K\cos\left(\sqrt{-\varpi}\phi\right) - \sqrt{-\varpi}\sin\left(\sqrt{-\varpi}\phi\right) - \sqrt{-\varpi}\right)}, \tag{42}$$

and

$$Q_{3,4}(t,x,y,z) = -\frac{m_1 K}{2} - \frac{m_1 \varpi \left(\sin\left(\sqrt{-\varpi}\phi\right) - 1\right)}{\cos\left(\sqrt{-\varpi}\phi\right)\left(K\cos\left(\sqrt{-\varpi}\phi\right) - \sqrt{-\varpi}\sin\left(\sqrt{-\varpi}\phi\right) + \sqrt{-\varpi}\right)}. \tag{43}$$

Family. 3.2: When $\varpi > 0 \quad L \neq 0$,

$$Q_{3,5}(t,x,y,z) = -\frac{m_1 K}{2} - \frac{m_1 \varpi \left(-1 + \left(\tanh\left(\frac{1}{2}\sqrt{\varpi}\phi\right)\right)^2\right)}{2(K + \sqrt{\varpi}\tanh\left(\frac{1}{2}\sqrt{\varpi}\phi\right))}, \tag{44}$$

$$Q_{3,6}(t,x,y,z) = -\frac{m_1 K}{2} - \frac{m_1 \varpi \left(-1 + i\sinh\left(\sqrt{\varpi}\phi\right)\right)}{\cosh\left(\sqrt{\varpi}\phi\right)\left(K\cosh\left(\sqrt{\varpi}\phi\right) + \sqrt{\varpi}\sinh\left(\sqrt{\varpi}\phi\right) + i\sqrt{\varpi}\right)}, \tag{45}$$

$$Q_{3,7}(t,x,y,z) = -\frac{m_1 K}{2} + \frac{m_1 \varpi \left(1 + i\sinh\left(\sqrt{\varpi}\phi\right)\right)}{\cosh\left(\sqrt{\varpi}\phi\right)\left(K\cosh\left(\sqrt{\varpi}\phi\right) + \sqrt{\varpi}\sinh\left(\sqrt{\varpi}\phi\right) - i\sqrt{\varpi}\right)}, \tag{46}$$

and

$$Q_{3,8}(t,x,y,z) = -\frac{m_1 K}{2} + \frac{m_1 \varpi \left(2\left(\cosh\left(\frac{1}{4}\sqrt{\varpi}\phi\right)\right)^2 - 1\right)}{4\left(\cosh\left(\frac{1}{4}\sqrt{\varpi}\phi\right)\sinh\left(\frac{1}{4}\sqrt{\varpi}\phi\right)\left(2K\cosh\left(\frac{1}{4}\sqrt{\varpi}\phi\right)\sinh\left(\frac{1}{4}\sqrt{\varpi}\phi\right) - \sqrt{\varpi}\right)\right)}. \tag{47}$$

Family. 3.3: When $\varpi = 0, \quad K \neq 0$,

$$Q_{3,9}(t,x,y,z) = -\frac{m_1 K}{2} - 2\frac{m_1}{\phi\,(K\phi + 2)}. \tag{48}$$

Family. 3.4: When $\varpi = 0$, in case when $K = L = 0$,

$$Q_{3,10}(t,x,y,z) = \frac{m_1}{\phi}. \tag{49}$$

Family. 3.5: When $\varpi = 0$, in case when $K = J = 0$,

$$Q_{3,11}(t,x,y,z) = -\frac{m_1}{\phi}. \tag{50}$$

Family. 3.6: When $K = \epsilon$, $J = \kappa\epsilon(\kappa \neq 0)$ and $L = 0$,

$$Q_{3,12}(t,x,y,z) = -\frac{m_1\epsilon}{2} + \frac{m_1\epsilon\, e^{\epsilon\,\phi}}{e^{\epsilon\,\phi} - \kappa}. \tag{51}$$

Family. 3.7: When $K = \epsilon$, $L = \kappa\epsilon(\kappa \neq 0)$ and $J = 0$,

$$Q_{3,13}(t,x,y,z) = -\frac{m_1\epsilon}{2} - \frac{m_1\epsilon}{-1 + \kappa\, e^{\epsilon\,\phi}}. \tag{52}$$

Family. 3.8: When $J = 0$, $L \neq 0$ and $K \neq 0$,

$$Q_{3,14}(t,x,y,z) = -\frac{m_1K}{2} + \frac{m_1K(\sinh(K\phi) - \cosh(K\phi))}{-\cosh(K\phi) + \sinh(K\phi) - n_2}, \tag{53}$$

and

$$Q_{3,15}(t,x,y,z) = -\frac{m_1K}{2} + \frac{m_1Kn_2}{\cosh(K\phi) + \sinh(K\phi) + n_2}. \tag{54}$$

In the above kink soliton solutions, $\phi = \lambda x + (\frac{-4(\lambda-\omega)}{(8JL+K^2)m_1{}^2})y + (\frac{2(\lambda-\omega)}{\lambda\,\omega\,(8JL+K^2)})z - \omega t$.

Taking into consideration **Case. 4** and utilizing (9) and (11) with the corresponding solution of (8), we acquire the ensuing families of kink soliton solutions for (4):
Family. 4.1: When $\varpi < 0 \quad L \neq 0$,

$$\begin{aligned} Q_{4,1}(t,x,y,z) = &-\frac{m_1K}{2} + \frac{m_1\varpi\left(1 + \left(\tan\left(\frac{1}{2}\sqrt{-\varpi}\phi\right)\right)^2\right)}{2(K - \sqrt{-\varpi}\tan\left(\frac{1}{2}\sqrt{-\varpi}\phi\right))} \\ &-m_1J\left(-\frac{K}{2L} + \frac{\sqrt{-\varpi}\tan\left(\frac{1}{2}\sqrt{-\varpi}\phi\right)}{2L}\right)^{-1}, \end{aligned} \tag{55}$$

$$\begin{aligned} Q_{4,2}(t,x,y,z) = &-\frac{m_1K}{2} + \frac{m_1\varpi\left(1 + \left(\cot\left(\frac{1}{2}\sqrt{-\varpi}\phi\right)\right)^2\right)}{2(K + \sqrt{-\varpi}\cot\left(\frac{1}{2}\sqrt{-\varpi}\phi\right))} \\ &-m_1J\left(-\frac{K}{2L} - \frac{\sqrt{-\varpi}\cot\left(\frac{1}{2}\sqrt{-\varpi}\phi\right)}{2L}\right)^{-1}, \end{aligned} \tag{56}$$

$$\begin{aligned} Q_{4,3}(t,x,y,z) = &\frac{m_1\varpi\left(1 + \sin\left(\sqrt{-\varpi}\phi\right)\right)}{\cos\left(\sqrt{-\varpi}\phi\right)\left(K\cos\left(\sqrt{-\varpi}\phi\right) - \sqrt{-\varpi}\sin\left(\sqrt{-\varpi}\phi\right) - \sqrt{-\varpi}\right)} \\ &- m_1J\left(-\frac{K}{2L} + \frac{\sqrt{-\varpi}\left(\tan\left(\sqrt{-\varpi}\phi\right) + \sec\left(\sqrt{-\varpi}\phi\right)\right)}{2L}\right)^{-1} - \frac{m_1K}{2}, \end{aligned} \tag{57}$$

and

$$Q_{4,4}(t,x,y,z) = -\frac{m_1\varpi\left(\sin\left(\sqrt{-\varpi}\phi\right)-1\right)}{\cos\left(\sqrt{-\varpi}\phi\right)\left(K\cos\left(\sqrt{-\varpi}\phi\right)-\sqrt{-\varpi}\sin\left(\sqrt{-\varpi}\phi\right)+\sqrt{-\varpi}\right)} - m_1 J\left(-\frac{K}{2L}+\frac{\sqrt{-\varpi}\left(\tan\left(\sqrt{-\varpi}\phi\right)-\sec\left(\sqrt{-\varpi}\phi\right)\right)}{2L}\right)^{-1} - \frac{m_1 K}{2}. \tag{58}$$

Family. 4.2: When $\varpi > 0 \quad L \neq 0$,

$$Q_{4,5}(t,x,y,z) = -\frac{m_1 K}{2} - \frac{m_1\varpi\left(-1+\left(\tanh\left(\frac{1}{2}\sqrt{\varpi}\phi\right)\right)^2\right)}{2(K+\sqrt{\varpi}\tanh\left(\frac{1}{2}\sqrt{\varpi}\phi\right))} - m_1 J\left(-\frac{K}{2L}-\frac{\sqrt{\varpi}\tanh\left(\frac{1}{2}\sqrt{\varpi}\phi\right)}{2L}\right)^{-1}, \tag{59}$$

$$Q_{4,6}(t,x,y,z) = -\frac{m_1\varpi\left(-1+i\sinh\left(\sqrt{\varpi}\phi\right)\right)}{\cosh\left(\sqrt{\varpi}\phi\right)\left(K\cosh\left(\sqrt{\varpi}\phi\right)+\sqrt{\varpi}\sinh\left(\sqrt{\varpi}\phi\right)+i\sqrt{\varpi}\right)} - m_1 J\left(-\frac{K}{2L}-\frac{\sqrt{\varpi}\left(\tanh\left(\sqrt{\varpi}\phi\right)+i\mathrm{sech}\left(\sqrt{\varpi}\phi\right)\right)}{2L}\right)^{-1} - \frac{m_1 K}{2}, \tag{60}$$

$$Q_{4,7}(t,x,y,z) = \frac{m_1\varpi\left(1+i\sinh\left(\sqrt{\varpi}\phi\right)\right)}{\cosh\left(\sqrt{\varpi}\phi\right)\left(K\cosh\left(\sqrt{\varpi}\phi\right)+\sqrt{\varpi}\sinh\left(\sqrt{\varpi}\phi\right)-i\sqrt{\varpi}\right)} - m_1 J\left(-\frac{K}{2L}-\frac{\sqrt{\varpi}\left(\tanh\left(\sqrt{\varpi}\phi\right)-i\mathrm{sech}\left(\sqrt{\varpi}\phi\right)\right)}{2L}\right)^{-1} - \frac{m_1 K}{2}, \tag{61}$$

and

$$Q_{4,8}(t,x,y,z) = \frac{m_1\varpi\left(2\left(\cosh\left(\frac{1}{4}\sqrt{\varpi}\phi\right)\right)^2-1\right)}{4(\cosh\left(\frac{1}{4}\sqrt{\varpi}\phi\right)\sinh\left(\frac{1}{4}\sqrt{\varpi}\phi\right)\left(2K\cosh\left(\frac{1}{4}\sqrt{\varpi}\phi\right)\sinh\left(\frac{1}{4}\sqrt{\varpi}\phi\right)-\sqrt{\varpi}\right))} - m_1 J\left(-\frac{K}{2L}-\frac{\sqrt{\varpi}\left(\tanh\left(\frac{1}{4}\sqrt{\varpi}\phi\right)-\coth\left(\frac{1}{4}\sqrt{\varpi}\phi\right)\right)}{4L}\right)^{-1} - \frac{m_1 K}{2}. \tag{62}$$

Family. 4.3: When $K = \epsilon$, $J = \kappa\epsilon(\kappa \neq 0)$ and $L = 0$,

$$Q_{4,9}(t,x,y,z) = -\frac{m_1\epsilon}{2} + \frac{m_1\epsilon\, e^{\epsilon\phi}}{e^{\epsilon\phi}-\kappa} - \frac{m_1\kappa\epsilon}{e^{\epsilon\phi}-\kappa}. \tag{63}$$

Family. 4.4: When $K = \epsilon$, $L = \kappa\epsilon(\kappa \neq 0)$ and $J = 0$,

$$Q_{4,10}(t,x,y,z) = -\frac{m_1\epsilon}{2} - \frac{m_1\epsilon}{-1+\kappa\, e^{\epsilon\phi}}. \tag{64}$$

**Family. 4.5**: When $J = 0$, $L \neq 0$ and $K \neq 0$,

$$Q_{4,11}(t,x,y,z) = -\frac{m_1 K}{2} + \frac{m_1 K(\sinh(K\phi)-\cosh(K\phi))}{-\cosh(K\phi)+\sinh(K\phi)-n_2}, \tag{65}$$

and

$$Q_{4,12}(t,x,y,z) = -\frac{m_1 K}{2} + \frac{m_1 K n_2}{\cosh(K\phi) + \sinh(K\phi) + n_2}. \tag{66}$$

In the above kink soliton solutions, $\phi = \lambda x + (\frac{-4(\lambda-\omega)}{\omega\, {m_1}^2})y + (\frac{2(\lambda-\omega)}{\lambda\,\omega\,\omega})z - \omega t$.

## 4. Results and Discussion

In this section, numerous traveling soliton structures discovered in the model under investigation are visually displayed. In the framework of WBBM, we use the innovative RMESEM to extract and depict a number of wave structures in 3D, 2D, and contour forms, exposing the presence of multiple kink solitons, including anti-kink, twinning kink, bright kink, bifurcated kink, lump-like kink, and other multiple kinks. Traveling wave solutions such as soliton types are crucial for understanding the dynamic behavior of many physical systems modeled by NPDEs. Self-reinforcing solitary waves, or soliton waves, are able to maintain their form during propagation. Their localized character and stability set them apart.

Prominently, we obtain kink solitons such as solitary kink, anti-kink, twinning kink, bright kink, bifurcated kink, lump-like kink and other multiple kinks in the realm of WBBM. A single, localized wave that keeps its form while moving at a steady pace is called a solitary kink. It symbolizes a single, steady crest or depression that travels across the water surface without altering shape in water ripples. A reversed version of an isolated kink, an anti-kink symbolizes a falling wave in a situation where a solitary kink represents a rising wave. It shows a depression or dip that moves steadily across the surface in the case of water surges. When two kinks move in tandem, they form a twinning kink, which frequently takes the form of two linked waves. This is a representation of two parallel troughs and crests moving across the surface of the water. A localized wave that is larger in frequency than the medium it surrounds is called a bright kink. It denotes a prominent, bright crest that moves with noticeable movement in surges of water. As it spreads, a bifurcated kink divides into multiple tendrils. When it comes to water crests, it is a situation in which an individual wave peak or depression splits, resulting in many wave fronts or pathways. A localized wave which looks a lump and bump, frequently in a three-dimensional in nature situation, is called a lump-like kink. This is an additional curved localized rise or dip in the waves of water as opposed to the crispness of a single kink. Finally, a sequence of kink oscillations engaging or passing through a medium is referred to as many kinks. When it comes to water gestures, they symbolize a complicated arrangement of several cresting and crashing points that move in tandem to form a complex waveform formation. Each of these kinds of waves demonstrates the many kinetics of the water propagation of waves and shows how the WBBM model may be used to predict and comprehend a wide range of complicated and diverse wave behaviors. Moreover, the graph for $Q_{1,5}$ in (20) displays the profile of the solitary kink soliton as seen in Figure 1. The graph for $Q_{1,9}$ in (24) is shown in Figure 2, which displays a bright kink soliton profile. Similarly, the graph for $Q_{2,5}$ given in (29) is displayed in Figure 3, which shows the anti-kink soliton profile. The graph for $Q_{2,11}$ given in (35) is displayed in Figure 4, which exhibits the bifurcated kink soliton profile. Figure 5 represents the graph for $Q_{2,14}$ shown in (38), which displays the soliton profile of a solitary kink. Likewise, Figure 6 shows the graph for $Q_{3,3}$ reported in (42), which displays a lump-like kink soliton profile. The graph for $Q_{3,8}$, which is a bright kink soliton profile, is shown in Figure 7. The graph of the twinning kink soliton profile is shown in Figure 8 for $Q_{3,9}$ as reported in (48). Figure 9 is plotted for $Q_{4,5}$ articulated in (59), which shows a solitary kink soliton profile. Finally, the graph for $Q_{4,10}$ given in (64) displays the kink soliton profile in Figure 10.

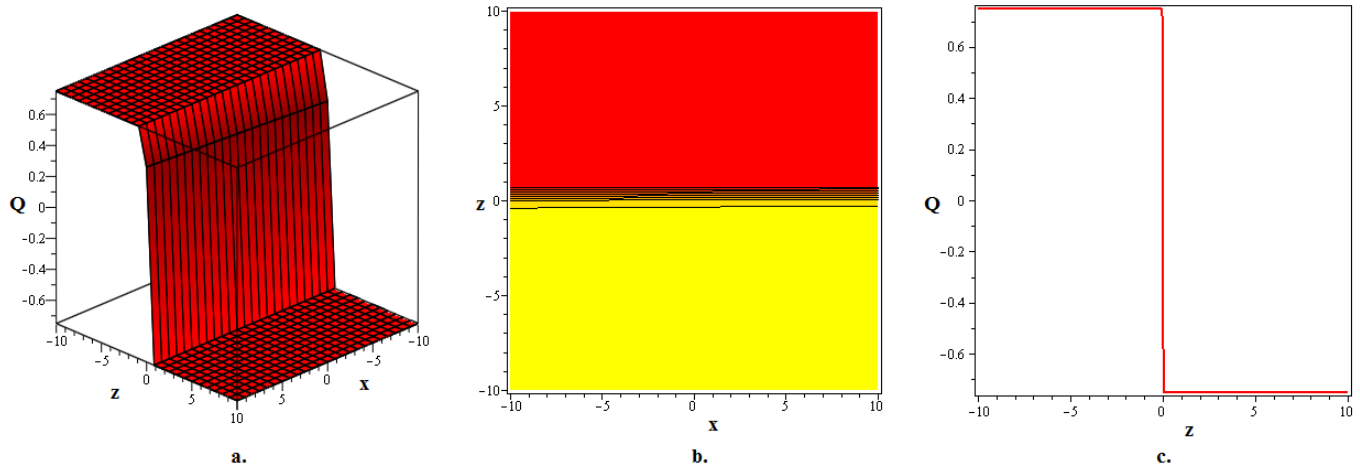



**Figure 1.** (**a**–**c**) The 3D, contour, and 2D (when $x = 1$) graphs for the solitary kink soliton solution $Q_{1,5}$ stated in (20) are plotted for $J = 2, K = 5, L = 2, \lambda = 0.005, \omega = 0.025, s_0 = 1, t = 0, y = 1$.

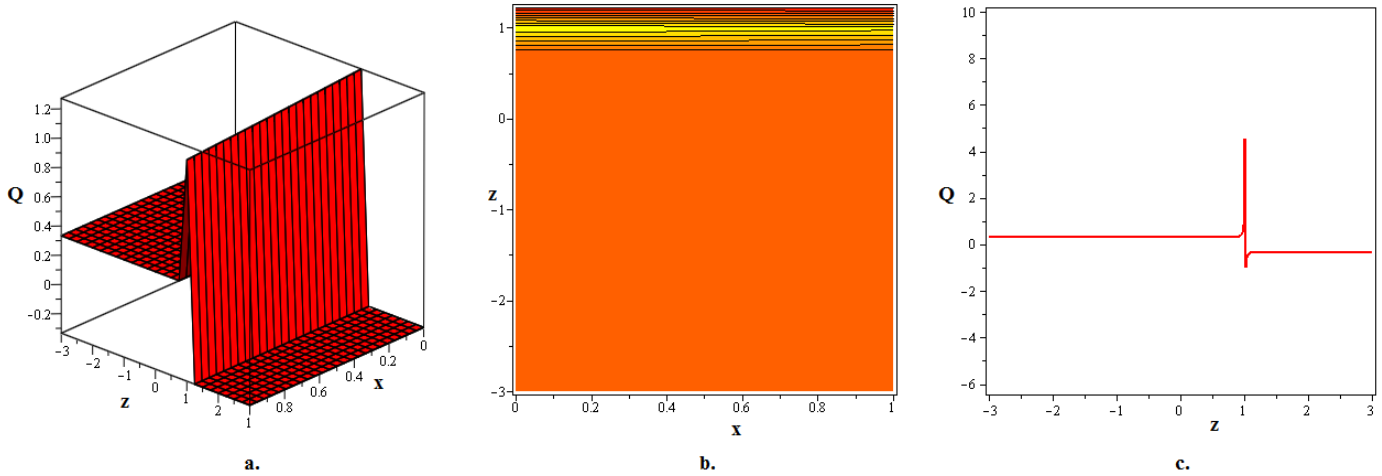



**Figure 2.** (**a**–**c**) The 3D, contour, and 2D (when $x = 2$) graphs for the bright kink soliton solution $Q_{1,9}$ stated in (24) are plotted for $J = 9, K = 3, L = 0, \lambda = 0.015, \omega = 0.35, s_0 = 2, t = 1, y = 5, \kappa = 3, \epsilon = 3$.

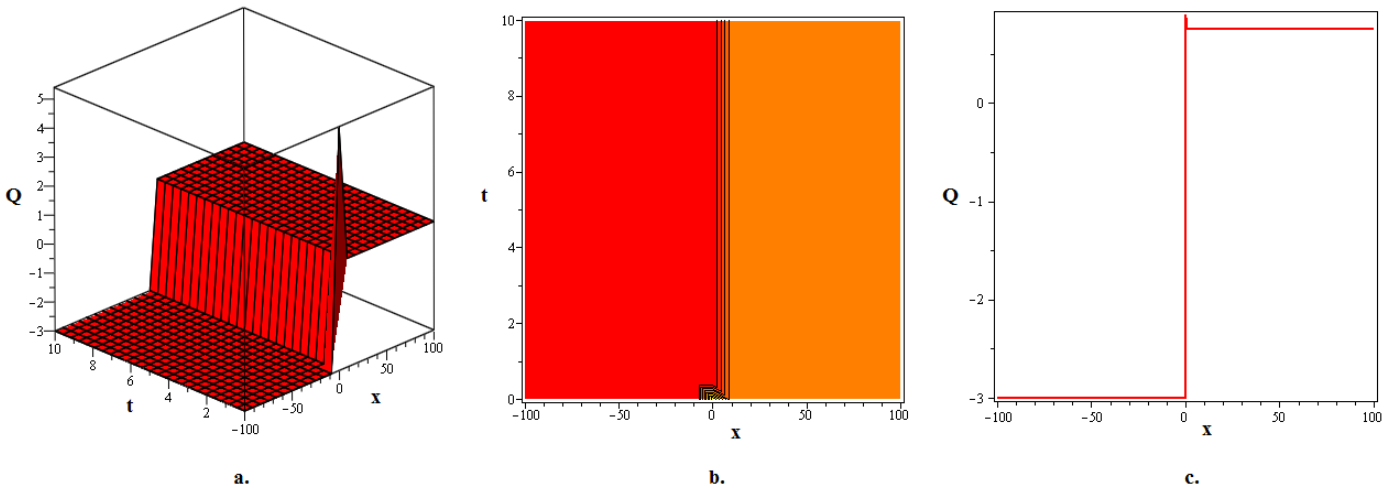



**Figure 3.** (**a**–**c**) The 3D, contour, and 2D (when $t = 1$) graphs for the anti-kink soliton solution $Q_{2,5}$ stated in (29) are plotted for $J = 8, K = 10, L = 2, \lambda = 50, \omega = 15, s_0 = 5, m_0 = 2, m_1 = 3$.

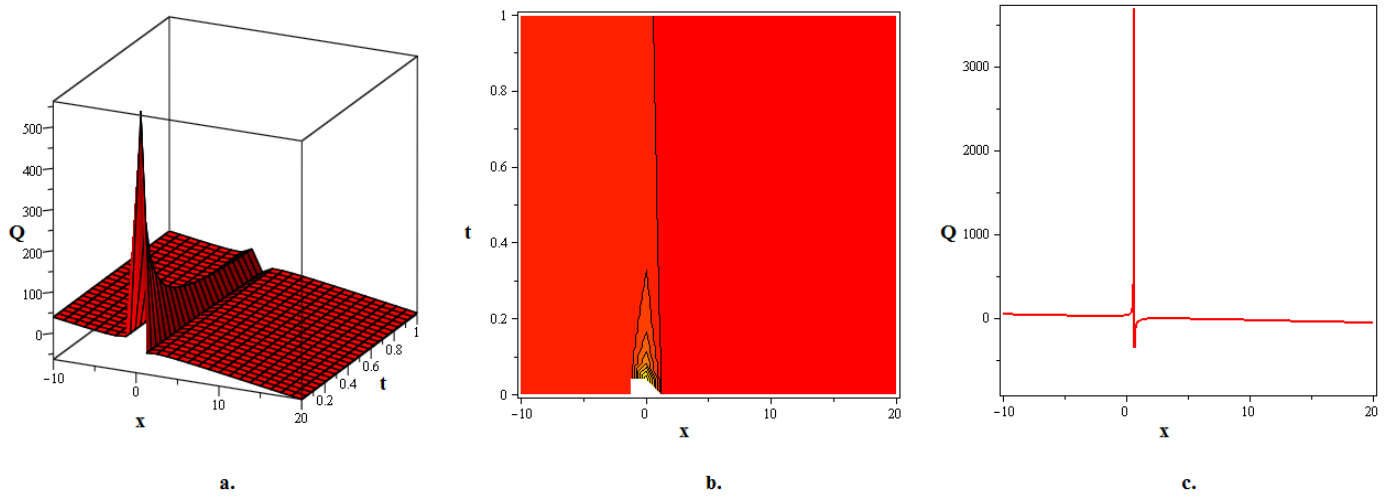



**Figure 4.** (**a**–**c**) The 3D, contour, and 2D (when $t = 1$) graphs for the bifurcated kink soliton solution $Q_{2,11}$ stated in (35) are plotted for $J = 0, K = 0, L = 1, \lambda = 0.335, \omega = 0.215, s_0 = 10, m_0 = 4, m_1 = 5$. In this profile, the kink interacts with shock wave.

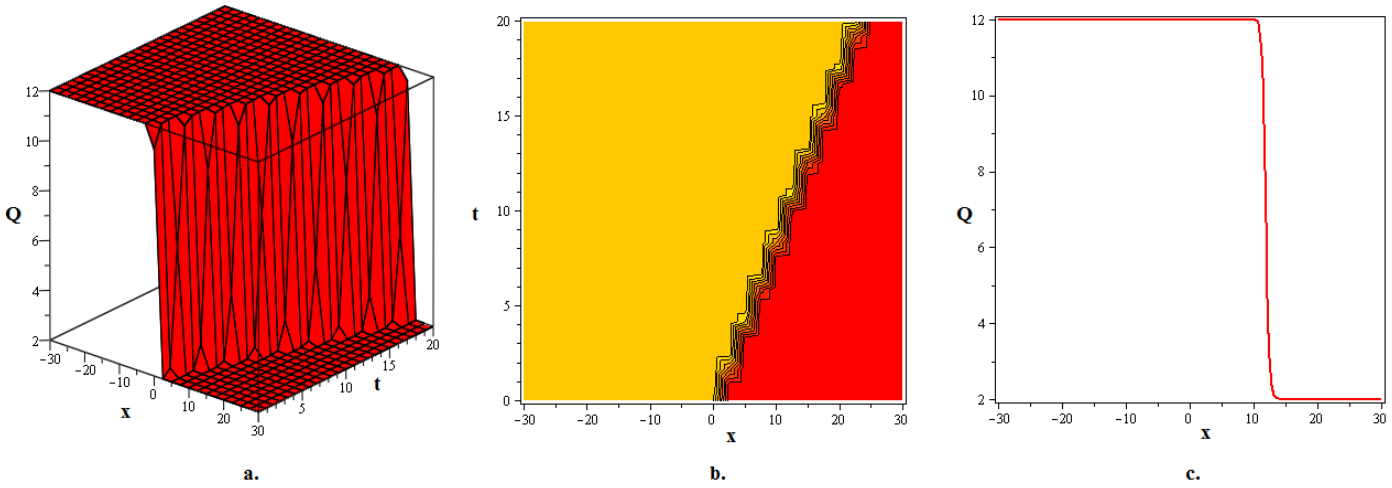



**Figure 5.** (**a**–**c**) The 3D, contour, and 2D (when $t = 10$) graphs for the solitary kink soliton solution $Q_{2,14}$ stated in (38) are plotted for $J = 0, K = 5, L = 0, \lambda = 0.75, \omega = 0.85, s_0 = 15, m_0 = 2, m_1 = 2, n_1 = 0.5, n_2 = 0.10$.

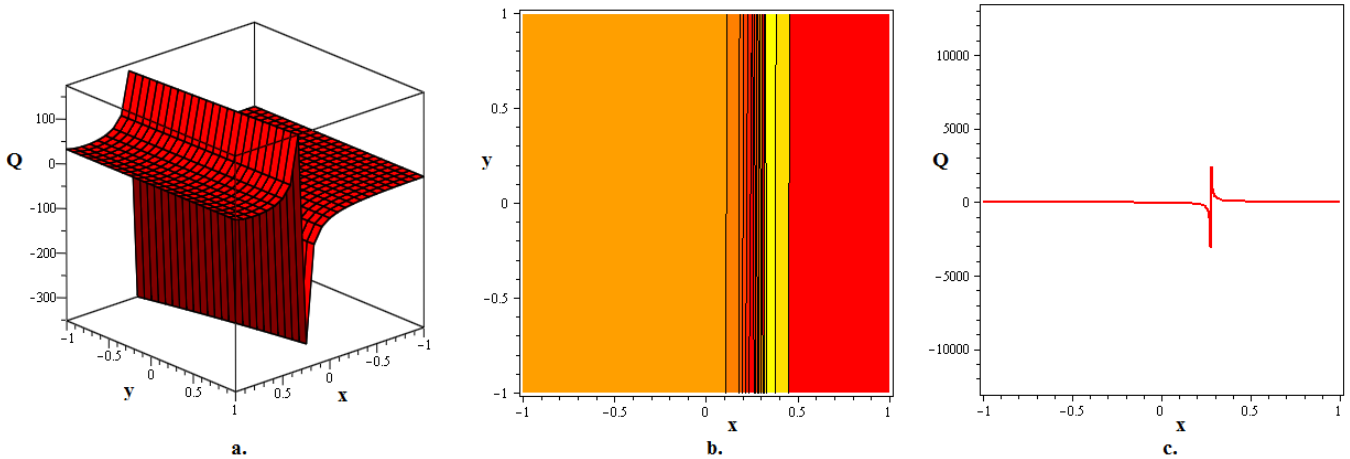



**Figure 6.** (**a**–**c**) The 3D, contour, and 2D (when $y = 0$) graphs for the lump-type kink soliton solution $Q_{3,3}$ stated in (42) are plotted for $J = 1, K = \sqrt{(7)}, L = 4, \lambda = 0.545, \omega = 0.235, m_1 = 5, t = 10, z = 0.5$.

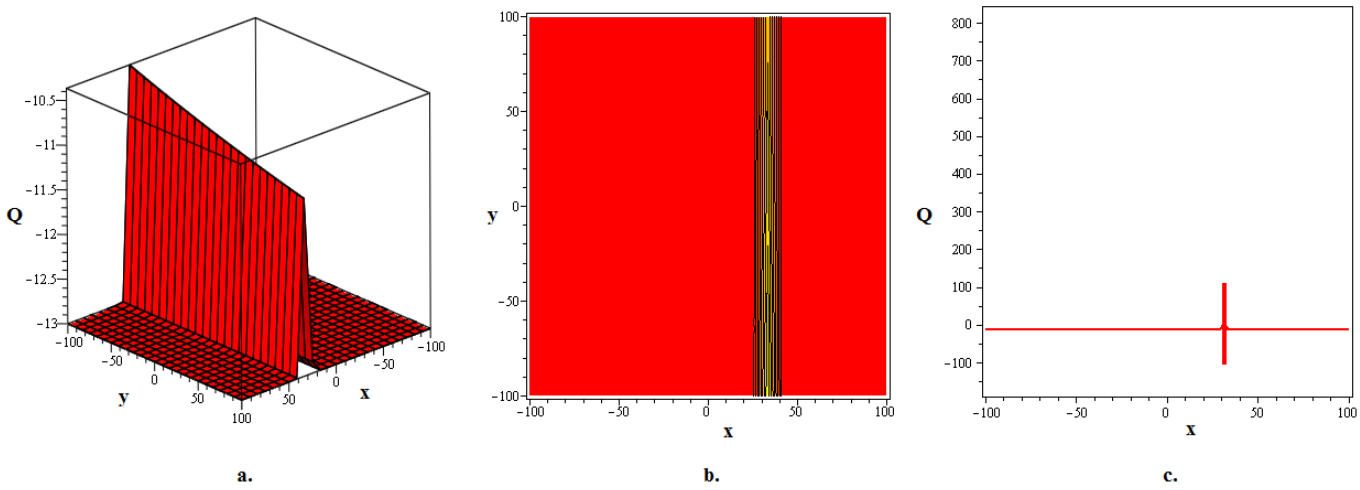



**Figure 7.** (**a**–**c**) The 3D, contour, and 2D (when $y = 20$) graphs for the bright kink soliton solution $Q_{3,8}$ stated in (47) are plotted for $J = 3, K = 13, L = 12, \lambda = 0.221, \omega = 0.345, m_1 = 2, t = 20, z = 1$.

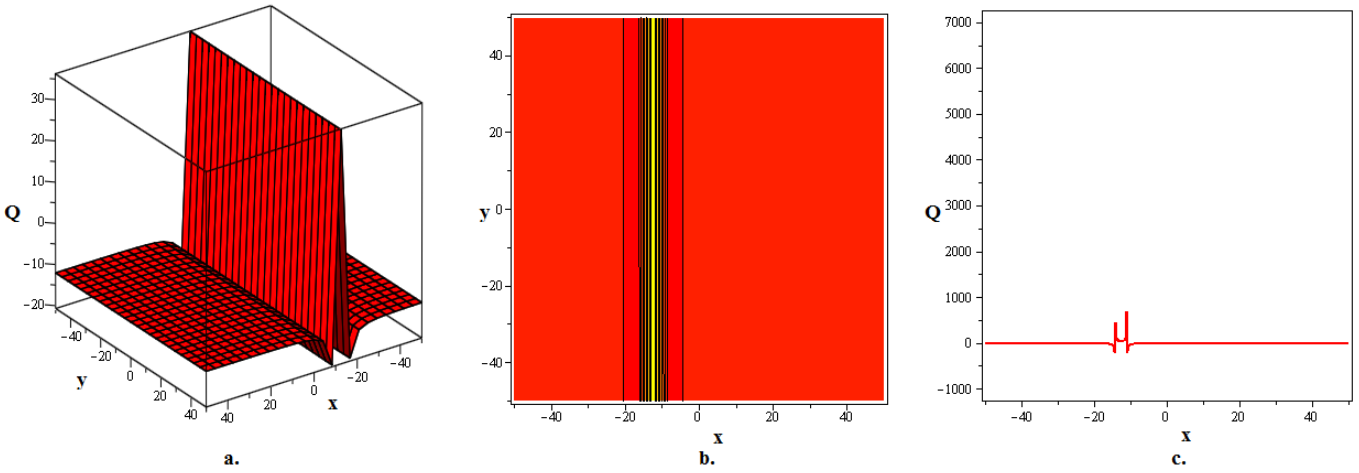



**Figure 8.** (**a**–**c**) The 3D, contour, and 2D (when $y = 0$) graphs for the twinning kink soliton solution $Q_{3,9}$ stated in (48) are plotted for $J = 1, K = 2, L = 1, \lambda = 0.315, \omega = 0.115, m_1 = 12, t = 10, z = 5$.

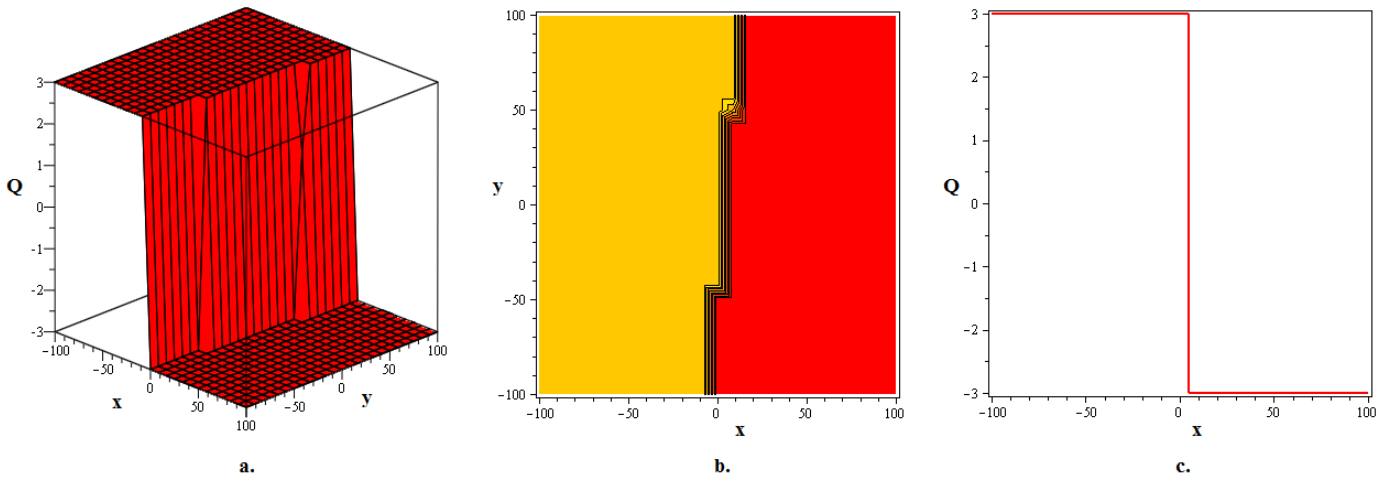



**Figure 9.** (**a**–**c**) The 3D, contour, and 2D (when $y = 10$) graphs for the multiple kink soliton solution $Q_{4,5}$ stated in (59) are plotted for $J = 4, K = 10, L = 4, \lambda = 5, \omega = 1, m_1 = 1, t = 20, z = 10$.

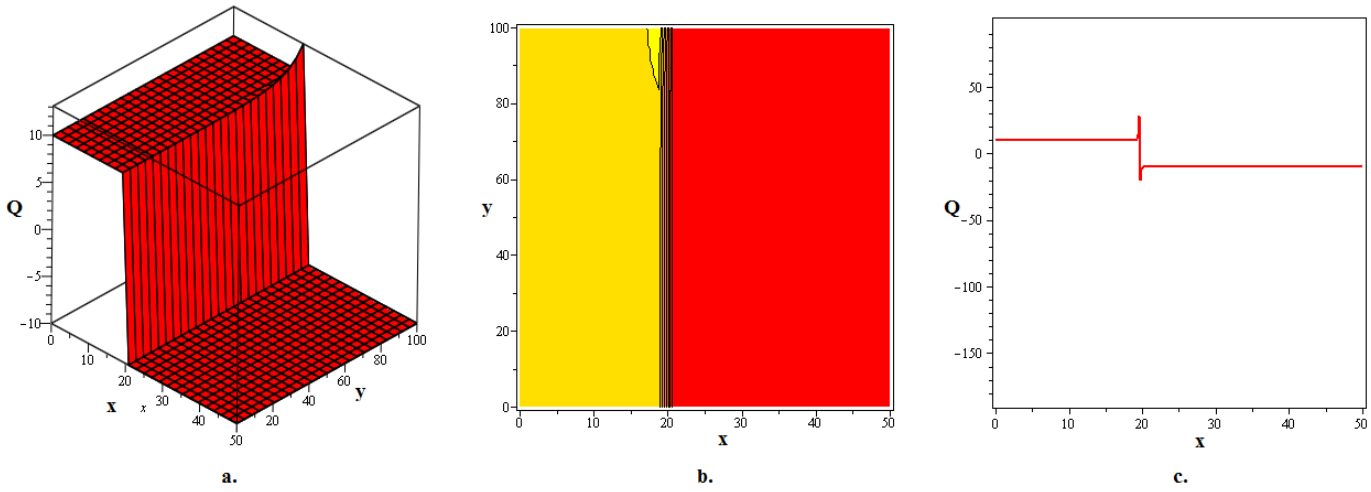



**Figure 10.** (**a**–**c**) The 3D, contour, and 2D (when $y = 30$) graphs for the kink soliton solution $Q_{4,10}$ stated in (64) are plotted for $J = 0, K = 10, L = 20, \lambda = 1, \omega = 2, m_1 = 2, t = 10, z = 2, \epsilon = 10, \kappa = 2$.

## 5. Conclusions

In conclusion, an innovative technique known as RMESEM is utilized in this study to produce and evaluate precise families of soliton solutions for the (3+1)-dimensional WBBM. The propagating behavior of acquired solitons is graphically represented by the 3D, 2D, and contour graphics, which clearly demonstrated the existence of several types of kink solitons in the setting of WBBM, including anti-kink, twinning kink, bright kink, bifurcated kink, lump-like kink, and other multiple kinks. The obtained soliton solutions provide insightful information on the WBBM model behavior. Moreover, it is demonstrated that solving NPDEs with the RMESEM approach is a flexible and effective strategy. Our understanding of the underlying physical processes and the relationships between different wave phenomena in a nonlinear setting are advanced by its ability to create a range of soliton families. Understanding the stability, interactions, and soliton dispersion aspects of the WBBM model is further made easier with the help of the derived soliton solutions. Nonetheless, the approach fails when the highest derivative term and nonlinear terms are not homogeneously balanced. Notwithstanding this limitation, the present investigation demonstrates that the methodology employed in this work is highly portable and efficacious for nonlinear problems in a variety of scientific domains. Moreover, further exploration into the stability analysis of solitons as well as the inclusion and effects of fractional derivatives on solitons within the context of targeted model is the future objective of this study.

**Author Contributions:** Conceptualization, M.Y.A.; Methodology, M.Y.A.; Validation, H.A.; Data curation, H.A. All authors have read and agreed to the published version of the manuscript.

**Funding:** This research received no external funding.

**Data Availability Statement:** The original contributions presented in the study are included in the article, further inquiries can be directed to the corresponding authors.

**Acknowledgments:** The authors gratefully acknowledge the funding of the Deanship of Graduate Studies and Scientific Research, Jazan University, Saudi Arabia, through project number: RG24-L02.

**Conflicts of Interest:** The authors declare no conflicts of interest.

## Appendix A

### *Appendix A.1. Comparison with Other Analytical Methods*

The findings of the other analytical procedures can be derived from our method. For example, setting $m_1 = 0$ in (11) results in

$$P(\phi) = s_0\left(\frac{1}{\Upsilon(\phi)}\right). \tag{A1}$$

This displays the EDAM closed-form solution's structure [29]. Thus, by setting $m_1 = 0$ from our findings, the results obtained by EDAM may also be achieved. For example, if we put $m_0 = a_0$, $s_0 = b_1$, $J = \Omega$, $K = 0$, and $L = 1$ as shown in (8), we receive some of the findings from our results gained under **Case. 1** that Shafqat-Ur-Rahman [37] achieved. In a similar manner, we obtain (11) if we set $s_0 = 0$:

$$P(\phi) = \sum_{m=0}^{1} m_j\left(\frac{\Upsilon'(\phi)}{\Upsilon(\phi)}\right)^j, \tag{A2}$$

which, using the Riccati-NODE, is the closed-form solution given by the (G′/G)-expansion technique [38]. Therefore, the results of EDAM and the (G′/G)-expansion approach may be more broadly obtained from the generalized results in our study.

*Appendix A.2. Fractional Generalization*

We may generalize our findings to the fractional form. As an example, let us consider the (4) with conformable derivatives of $\delta$-order, i.e.,

$$D_t^\delta Q + D_x^\delta Q + D_y^\delta Q^3 - D_{xzt}^{3\delta} Q = 0, \tag{A3}$$

then, all of our solutions are also those of Conformable WBBM (CWBBM) in (A3), where $\phi$ is defined as follows:

$$\phi = \frac{\lambda x^\delta}{\delta} + \frac{\mu y^\delta}{\delta} + \frac{\nu z^\delta}{\delta} - \frac{\omega t^\delta}{\delta}. \tag{A4}$$

## References


1. El-Ajou, A.; Arqub, O.A.; Momani, S. Approximate analytical solution of the nonlinear fractional KdV-Burgers equation: A new iterative algorithm. *J. Comput. Phys.* **2015**, *293*, 81–95. [CrossRef]
2. Alyobi, S.; Shah, R.; Khan, A.; Shah, N.A.; Nonlaopon, K. Fractional Analysis of Nonlinear Boussinesq Equation under Atangana-Baleanu-Caputo Operator. *Symmetry* **2022**, *14*, 2417. [CrossRef]
3. Khader, M.M.; Saad, K.M. A numerical study by using the Chebyshev collocation method for a problem of biological invasion: Fractional Fisher equation. *Int. J. Biomath.* **2018**, *11*, 1850099. [CrossRef]
4. Ma, H.C.; Peng, X.F.; Yao, D.D. Improved hyperbolic function method and exact solutions for variable coefficient Benjamin-Bona-Mahony-Burgers equation. *Therm. Sci.* **2015**, *19*, 1183–1187. [CrossRef]
5. Klein, C.; Sparber, C.; Markowich, P. Numerical study of fractional nonlinear Schrödinger equations. *Proc. R. Soc. Math. Phys. Eng. Sci.* **2014**, *470*, 20140364. [CrossRef] [PubMed]
6. Zhao, X.; Xu, W. Travelling wave solutions for a class of the generalized Benjamin-Bona-Mahoney equations. *Appl. Math. Comput.* **2007**, *192*, 507–519. [CrossRef]
7. Nagatani, T. Modified KdV equation for jamming transition in the continuum models of traffic. *Phys. Stat. Mech. Its Appl.* **1998**, *261*, 599–607. [CrossRef]
8. Yusufoğlu, E.; Bekir, A. Exact solutions of coupled nonlinear evolution equations. *Chaos Solitons Fractals* **2008**, *37*, 842–848. [CrossRef]
9. Yavuz, M.; Abdeljawad, T. Nonlinear regularized long-wave models with a new integral transformation applied to the fractional derivative with power and Mittag-Leffler kernel. *Adv. Differ. Equ.* **2020**, *2020*, 367. [CrossRef]
10. Benjamin, T.B. *Lectures on Nonlinear Wave Motion*; Lecture Notes in Applied Mathematics; American Mathematical Society: Providence, RI, USA, 1974; Volume 15, pp. 3–47.
11. Kuru, S. Compactons and kink-like solutions of BBM-like equations by means of factorization. *Chaos Solitons Fractals* **2009**, *42*, 626–633. [CrossRef]
12. Wazzan, L. A modified tanh-coth method for solving the KdV and the KdV-Burgers' equations. *Commun. Nonlinear Sci. Numer. Simul.* **2009**, *14*, 443–450. [CrossRef]
13. Martynenko, A.; Chen, Y. Degradation kinetics of total anthocyanins and formation of polymeric color in blueberry hydrothermodynamic (HTD) processing. *J. Food Eng.* **2016**, *171*, 44–51. [CrossRef]
14. Davidson, P.A. An Introduction to Magnetohydrodynamics. *Am. J. Phys.* **2002**, *70*, 781. [CrossRef]
15. Bona, J.L.; Dougalis, V.A. An initial-and boundary-value problem for a model equation for propagation of long waves. *J. Math. Anal. Appl.* **1980**, *75*, 503–522. [CrossRef]

16. Bhimani, D.G.; Haque, S. Norm Inflation for Benjamin-Bona-Mahony Equation in Fourier Amalgam and Wiener Amalgam Spaces with Negative Regularity. *Mathematics* **2021**, *9*, 3145. [CrossRef]
17. Yokus, A.; Sulaiman, T.A.; Bulut, H. On the analytical and numerical solutions of the Benjamin-Bona-Mahony equation. *Opt. Quantum Electron.* **2018**, *50*, 31. [CrossRef]
18. Sahoo, S.; Saha Ray, S. A novel approach for stochastic solutions of wick-type stochastic time-fractional Benjamin-Bona-Mahony equation for modeling long surface gravity waves of small amplitude. *Stoch. Anal. Appl.* **2019**, *37*, 377–387. [CrossRef]
19. Rizvi, S.T.; Seadawy, A.R.; Ahmed, S.; Younis, M.; Ali, K. Study of multiple lump and rogue waves to the generalized unstable space time fractional nonlinear Schrödinger equation. *Chaos Solitons Fractals* **2021**, *151*, 111251. [CrossRef]
20. Darvishi, M.T.; Najafi, M.; Wazwaz, A.M. Soliton solutions for Boussinesq-like equations with spatio-temporal dispersion. *Ocean. Eng.* **2017**, *130*, 228–240. [CrossRef]
21. Ali, R.; Barak, S.; Altalbe, A. Analytical study of soliton dynamics in the realm of fractional extended shallow water wave equations. *Phys. Scr.* **2024**, *99*, 065235. [CrossRef]
22. Shah, R.; Hyder, A.A.; Iqbal, N.; Botmart, T. Fractional view evaluation system of Schrödinger-KdV equation by a comparative analysis. *AIMS Math.* **2022**, *7*, 19846–19864. [CrossRef]
23. Hammad, M.M.A.; Shah, R.; Alotaibi, B.M.; Alotiby, M.; Tiofack, C.G.L.; Alrowaily, A.W.; El-Tantawy, S.A. On the modified versions of (G′/G)-expansion technique for analyzing the fractional coupled Higgs system. *AIP Adv.* **2023**, *13*, 105131. [CrossRef]
24. Lou, S.Y.; Chen, L.L. Formal variable separation approach for nonintegrable models. *J. Math. Phys.* **1999**, *40*, 6491–6500. [CrossRef]
25. Alipour, M.M.; Domairry, G.; Davodi, A.G. An application of exp-function method to approximate general and explicit solutions for nonlinear Schrödinger equations. *Numer. Methods Partial. Differ. Equ.* **2011**, *27*, 1016–1025. [CrossRef]
26. Yang, X.J. A new integral transform method for solving steady heat-transfer problem. *Therm. Sci.* **2016**, *20* (Suppl. S3), 639–642. [CrossRef]
27. Alshehry, A.S.; Yasmin, H.; Shah, R. A homotopy perturbation method with Elzaki transformation for solving the fractional Biswas-Milovic model. *Open Phys.* **2023**, *21*, 20230147. [CrossRef]
28. Odibat, Z.; Momani, S.; Erturk, V.S. Generalized differential transform method: Application to differential equations of fractional order. *Appl. Math. Comput.* **2008**, *197*, 467–477. [CrossRef]
29. Noor, S.; Alyousef, H.A.; Shafee, A.; Shah, R.; El-Tantawy, S.A. A novel analytical technique for analyzing the (3+1)-dimensional fractional calogero-bogoyavlenskii-schiff equation: Investigating solitary/shock waves and many others physical phenomena. *Phys. Scr.* **2024**, *99*, 065257. [CrossRef]
30. Ali, R.; Kumar, D.; Akgül, A.; Altalbe, A. On the periodic soliton solutions for fractional schrodinger equations. *Fractals* **2024**, 32, 2440033. [CrossRef]
31. Bilal, M.; Iqbal, J.; Ali, R.; Awwad, F.A.; Ismail, E.A.A. Exploring Families of Solitary Wave Solutions for the Fractional Coupled Higgs System Using Modified Extended Direct Algebraic Method. *Fractal Fract.* **2023**, *7*, 653. [CrossRef]
32. Ali, R.; Hendy, A.S.; Ali, M.R.; Hassan, A.M.; Awwad, F.A.; Ismail, E.A. Exploring Propagating Soliton Solutions for the Fractional Kudryashov-Sinelshchikov Equation in a Mixture of Liquid-Gas Bubbles under the Consideration of Heat Transfer and Viscosity. *Fractal Fract.* **2023**, *7*, 773. [CrossRef]
33. Mohammed, F.A.; Elboree, M.K. Soliton solutions and periodic solutions for two models arises in mathematical physics. *AIMS Math.* **2021**, *7*, 4439–4458. [CrossRef]
34. Asjad, M.I.; Majid, S.Z.; Faridi, W.A.; Eldin, S.M. Sensitive analysis of soliton solutions of nonlinear Landau-Ginzburg-Higgs equation with generalized projective Riccati method. *AIMS Math.* **2023**, *8*, 10210–10227. [CrossRef]
35. Kuo, C.K.; Kumar, D.; Juan, C.J. A study of resonance Y-type multi-soliton solutions and soliton molecules for new (2+1)-dimensional nonlinear wave equations. *AIMS Math.* **2022**, *7*, 20740–20751. [CrossRef]
36. Xiao, Y.; Barak, S.; Hleili, M.; Shah, K. Exploring the dynamical behaviour of optical solitons in integrable kairat-II and kairat-X equations. *Phys. Scr.* **2024**, *99*, 095261. [CrossRef]
37. Bilal, M.; Ahmad, J. New exact solitary wave solutions for the 3D-FWBBM model in arising shallow water waves by two analytical methods. *Results Phys.* **2021**, *25*, 104230.
38. Akbar, M.A.; Ali, N.H.M.; Mohyud-Din, S.T. The alternative (G′/G)-expansion method with generalized Riccati equation: Application to fifth order (1+ 1)-dimensional Caudrey-Dodd-Gibbon equation. *Int. J. Phys. Sci.* **2012**, *7*, 743–752.


**Disclaimer/Publisher's Note:** The statements, opinions and data contained in all publications are solely those of the individual author(s) and contributor(s) and not of MDPI and/or the editor(s). MDPI and/or the editor(s) disclaim responsibility for any injury to people or property resulting from any ideas, methods, instructions or products referred to in the content.